



H₂S donor GYY4137 ameliorates paclitaxel-induced neuropathic pain in mice

Bedoor Qabazard^{a,*}, Willias Masocha^a, Maitham Khajah^a, Oludotun Adebayo Phillips^b

^a Department of Pharmacology and Therapeutics, Faculty of Pharmacy, Kuwait University, Kuwait

^b Department of Pharmaceutical Chemistry, Faculty of Pharmacy, Health Sciences Centre, Kuwait University, Kuwait



ARTICLE INFO

Keywords:

Hydrogen sulfide

Paclitaxel

Chemotherapy-induced neuropathic pain

ABSTRACT

Paclitaxel-induced neuropathic pain (PINP) is a dose-limiting side effect that largely affects the patient's quality of life and may limit the use of the drug as a chemotherapeutic agent for treating metastatic breast cancer and other solid tumors. Recently, a putative role for the gaseous mediator hydrogen sulfide (H₂S) in nociception modulation has been suggested. The aim of the present study was to investigate the potential efficacy of the slow release H₂S donor GYY4137 to alleviate and prevent PINP. Female BALB/c mice that were intraperitoneally (i.p.) injected with paclitaxel (2 mg/kg) for 5 consecutive days developed thermal hyperalgesia, cold and mechanical allodynia and had reduced of H₂S, generation in the spinal cord and paw skin. Treatment of mice with established thermal hyperalgesia with GYY4137 or the analgesic positive control drug gabapentin produced anti-hyperalgesic activities. The antihyperalgesic activity of GYY4137 was antagonized by the ATP sensitive potassium channels (K_{ATP} channels) blocker glibenclamide. Co-treatment with GYY4137 and paclitaxel prevented the paclitaxel-induced decrease in H₂S, generation as well as the paclitaxel-induced thermal hyperalgesia, cold allodynia and mechanical allodynia. GYY4137 enhanced paclitaxel's anti-proliferative effects against the breast cancer cell line MCF-7. The present results suggest that GYY4137 alleviates paclitaxel-induced thermal hyperalgesia, via K_{ATP} channels. GYY4137 prevents PINP possibly by blocking the paclitaxel-induced reduction in the generation of H₂S, in the tissues, while enhancing the anti-cancer activity of paclitaxel, and therefore warrants further research as a candidate for prevention of PINP in clinical settings.

1. Introduction

Platinum analogues (cisplatin and oxaliplatin), taxanes (paclitaxel), vinca alkaloids (vincristine) and proteasome inhibitors (bortezomib) are the most common antineoplastic drugs successfully employed as first-line treatment for several solid and blood cancers, including breast, lung, colorectal, gastric cancers and multiple myeloma. Although these compounds have different chemical structures and mechanisms of action, they all induce the development of chemotherapy-induced neuropathic pain (CINP) as a common side effect. Some of the symptoms of neuropathic pain include hyperalgesia (an increased response to normally painful stimuli), allodynia (pain triggered by normally non-painful stimuli, such as cloth rubbing against the skin) and spontaneous sensations such as burning, shooting, numbness, spasm and prickling [1,2]. These symptoms can have a serious negative impact on the psychosocial well-being and overall quality of life of the patient. Unfortunately, there are no clinically proven effective drugs for the prevention of CINP. A variety of therapeutic agents are used to relieve

patients with CINP [3], but currently only duloxetine has moderate recommendation for the treatment of CINP [4,5]. The gaseous signaling molecule hydrogen sulfide (H₂S) has recently been proposed to play a role as neuromodulator and cytoprotective mediator in several tissues, including the cardiovascular and nervous system [6–8]. A putative role for H₂S in nociception modulation has been suggested. For example, inhaled H₂S has been shown to prevent the neuropathic pain behavior induced by chronic constriction injury of the sciatic nerve in mice [9] and rats [10]. Moreover, H₂S-releasing analgesic compounds have been shown to exert greater potency against different forms of pain [11]. Furthermore, H₂S has been shown to induce mu opioid receptor-dependent analgesia in a rodent model of visceral pain [12]. A recent study showed a role of H₂S donors in relieving established CINP possibly via activation of voltage-gated Kv7potassium channels [13], however whether there are changes in H₂S during CINP, H₂S donors can prevent the development of CINP or other potassium channels play a role in the activity of H₂S donors against CINP remains to be identified. The aims of this study were therefore to evaluate the whether GYY4137

* Corresponding author.

E-mail address: bedoor.qabazard@hsc.edu.kw (B. Qabazard).

<https://doi.org/10.1016/j.bioph.2020.110210>

Received 16 February 2020; Received in revised form 25 April 2020; Accepted 28 April 2020

0753-3322/ © 2020 The Authors. Published by Elsevier Masson SAS. This is an open access article under the CC BY-NC-ND license (<http://creativecommons.org/licenses/by-nc-nd/4.0/>).

can prevent the development of PINP and alleviate established paclitaxel-induced thermal hyperalgesia (therapeutic regimen), whether K_{ATP} channels are involved in the antihyperalgesic effect of GYY4137, and whether there are changes in H_2S levels or generation capacity in tissues during PINP.

2. Materials and methods

2.1. Drugs and chemicals

Paclitaxel was purchased from Tocris Bioscience (Cat. No. 1097; Bristol, UK), and all other drugs were purchased from Sigma Aldrich, St. Louis, MO, except GYY4137 which was synthesized in-house, as described by Li et al. [15]. Structural characterization by spectrometric methods was performed by The General Facilities Science (GF-S), Faculty of Science, Kuwait University, Kuwait. Briefly, GYY4137 was synthesized as follows: Morpholine (40 mmol) in anhydrous dichloromethane (DCM, 12 mL) was added dropwise to a solution of Lawesson's reagent (8.0 mmol) in anhydrous DCM (12 mL) under nitrogen gas at room temperature and the reaction mixture was stirred for 2 h. The resulting precipitate was collected by suction filtration and washed several times with anhydrous DCM and dried to give a pure white solid product (66 % yield; melting point 156–159 °C). After synthesis, the purity and structure of the product were verified using Proton Nuclear Magnetic Resonance Spectrometry (1H NMR) and Mass Spectrometry. GYY4137 was analyzed by 1H -NMR spectrum in $CHCl_3$ - d_3 recorded on a Bruker Avance II 600 NMR spectrometer using solvent peak as a reference signal, and the Mass spectrum was recorded on a Waters QToF high resolution / Mass Spectrometer (LC-MS/MS High resolution). 1H -NMR (600 MHz; $CDCl_3$): δ 2.94–2.97 (4H, broad apparent q, $J = 6.0$ Hz, $N(CH_2)_2$ for morpholine attached to P), 3.19 (4H, broad t, $J = 4.9$ Hz, morpholinium $(CH_2)_2N$), 3.59 (4H, broad t, $J = 4.3$ Hz, $O(CH_2)_2$ for morpholine attached to P), 3.74 (4H, broad t, $J = 4.90$ Hz, morpholinium $(CH_2)_2O$), 3.82 (3H, s, CH_3O), 5.28 (1H , s, 0.5 CH_2Cl_2), 6.87–6.89 (2H, m, arylC-H o-to OCH3) and 8.15–8.05 (2H, m, arylC-H o-to P). 9.19 (2H, broad signal, morpholinium $+NH_2$). HRMS (m/z , ES $^+$): Calcd for $C_{15}H_{25}N_2O_3PS_2$ 376.1044; found 377.1100 ($M^+ + H$).

2.2. Animals and ethics statements

Female BALB/c mice (8–12 weeks old), weighing approximately 20–30 g, supplied by the Animal Resource Center (ARC) at the Health Sciences Center, Kuwait University were used in this study. All animals were housed under optimal laboratory conditions, maintained on a natural light and dark cycle and had free access to food and water ad libitum. Animals were acclimatized to laboratory conditions before any tests. All experimental procedures were carried out in strict accordance with the recommendations in the Guide for the Care and Use of Laboratory Animals of the National Institutes of Health (NIH Publication number 85–23, Revised 1985) as approved by the Animal Welfare and Ethics Committees of Kuwait University. Animals were handled in compliance with ethical guidelines for research in experimental pain with conscious animals [15], and all efforts were made to minimize suffering. Whenever possible, animal studies are reported in accordance with ARRIVE guidelines [16].

2.3. Induction of neuropathic pain by paclitaxel administration

Peripheral painful neuropathy was induced in mice by intraperitoneal (i.p.) administration of paclitaxel as previously described [17]. Paclitaxel was dissolved in a solution made up of 50 % Cremophor EL and 50 % absolute ethanol to a concentration of 6 mg/ml (stored at -20 °C, for a maximum of 14 days) and then diluted in normal saline (NaCl 0.9 %) to a final concentration of 0.2 mg/ml just before administration. The vehicle for paclitaxel was diluted at the time of injection

with normal saline in the same proportion as the paclitaxel solution, thus, constituted of about 1.7 % Cremophor EL and 1.7 % ethanol in normal saline. Paclitaxel (2 mg/kg) or its vehicle was administered to mice intraperitoneally (i.p.), in a volume of 10 mL/kg, once daily for 5 consecutive days. This treatment regimen has been reported to produce painful neuropathy and thermal hyperalgesia in mice [17–19]

2.4. Animal groups and treatment regimens

2.4.1. Acute (therapeutic) regimen

Mice were treated i.p. with GYY4137 (25, 50 and 100 mg/kg), gabapentin (10 mg/kg), used as an analgesic positive control as described previously [20], or vehicle once on day 7 after first administration of paclitaxel, when the mice had developed thermal hyperalgesia as previously described [17]. Reaction latencies to the hot plate test were measured before drug treatment (two baseline values) and at 0.5, 1, 1.5, 2, and 3 h post drug treatment.

2.4.2. Chronic (prophylactic) regimen

GYY4137 50 mg/kg was co-administered with paclitaxel daily for 5 days. The mice were assessed for the development of PINP using the hot and cold plate tests and dynamic plantar aesthesiometer.

2.5. Assessment of thermal nociception

For thermal hyperalgesia assessment, animals were individually placed on a hot-plate (Panlab S.L., Barcelona, Spain) with the temperature adjusted to 55 ± 1 °C. The latency to the first sign of paw licking, vocalization or jump response to avoid the heat was taken as an index of pain threshold. Reduction in paw licking or jump response time latency (RTL) indicates hyperalgesia, whereas an increase in RTL after drug treatment indicates antinociceptive activity of the drug. Reaction latencies to hot plate test were measured before (baseline latency), at day 7 after first injection of paclitaxel, and at various time points after drug treatment. A cut-off period of 20 s was maintained to avoid damage to the paws. For thermal allodynia test, animals were individually placed on a cold-plate with the temperature adjusted to 4 ± 1 °C. The latency to the first sign of paw licking was taken as an index of pain threshold. Reduction in paw licking RTL indicates allodynia, whereas an increase in RTL after drug treatment indicates antinociceptive activity of the drug. A cut-off period of 60 s was maintained to avoid damage to the paws.

2.6. Assessment of mechanical allodynia

Mechanical allodynia in mice was measured using the dynamic plantar aesthesiometer (Ugo Basile, Italy). Briefly, mice were left to habituate for 30 min inside plastic enclosures on top of a perforated platform before starting a microprocessor which was programmed to automatically lift a metal filament that exerted a linearly increasing force (0.25 g/s with cut-off time of 20 s) on the hind paw. A stop signal was automatically attained, either when the animal removed the paw or at the cut-off force of 5 g. Withdrawal thresholds in response to the mechanical stimulus were automatically recorded in grams. The hind paws were tested at least 3 times. The baseline mechanical threshold was assessed one day before the induction of the neuropathic pain.

2.7. Involvement of ATP sensitive potassium channel (K_{ATP} channel)

To explore the possible contribution of K_{ATP} channel in the antinociceptive effect of GYY4137, mice with paclitaxel-induced neuropathic pain were pre-treated with glibenclamide (an ATP-sensitive K $^+$ channel inhibitor) 15 min before the injection of either vehicle, or GYY4137 (50 mg/kg, i.p.). The reaction latencies to the hot plate were recorded at 2 h after injection of GYY4137 or vehicle.

2.8. Measurement of plasma H₂S level

H₂S levels were determined by zinc trapping spectrophotometric assay [14]. Blood samples were collected by cardiac puncture under terminal anesthesia and plasma was separated. The initial reaction mixture was made by mixing 50 μ l plasma with 200 μ l of 1 % zinc acetate. Then, 200 μ l of *N,N*-dimethyl-*p*-phenylenediamine sulfate (20 mM in 7.2 M HCl) and 200 μ l of FeCl₃ (30 mM in 1.2 M HCl) were added. After 10-minute incubation, the absorbance of the reaction mixture was measured at 670 nm, and H₂S concentration was calculated against a standard curve of NaHS solution (25–200 μ M).

2.9. Measurement of H₂S tissue synthesizing activity

Enzymatic H₂S synthesis in tissue homogenates was measured by zinc trapping spectrophotometric assay as described previously [14] with slight modification. Supernatant derived from the tissue homogenates (430 μ l) was incubated with 20 μ l pyridoxal 5'-phosphate (PLP, 2 mM) and the substrate L-cysteine (20 μ l, 10 mM) and sealed with a double parafilm layer to avoid leakage of H₂S gas generated after incubating the tube in a 37 °C water bath for 45 min. Baseline controls that contained trichloroacetic acid (TCA; 10 % w/v, 250 μ l) were prepared in parallel to obtain the basal H₂S background level. At the end of the incubation period, zinc acetate (1% w/v, 250 μ l) was injected to trap the H₂S followed by TCA (10 % w/v, 250 μ l) to terminate the reaction. Subsequently, *N,N*-dimethyl-*p*-phenylenediamine sulfate dye (NNDPD; 20 mM, 133 μ l) in 7.2 M HCl was added, followed by the addition of FeCl₃ (30 mM, 133 μ l) in 1.2 M HCl. After centrifugation (14,000 rpm for 4 min at 4 °C), absorbance (670 nm) of the resulting methylene blue in the supernatant was measured using a 96-well microplate reader (Tecan Systems Inc., CA, USA) and compared against a standard curve of NaHS (concentrations ranging from 3.125–250 μ M). At least 3 biological samples were assayed in duplicate and results were expressed as nmol H₂S formed per mg protein. Protein level in each homogenate was estimated using Bradford assay (Bio-Rad, CA, USA).

2.10. Anti-proliferative activity of GYY4137 and paclitaxel against breast cancer cell lines

Human breast carcinoma cell line MCF-7 (American Type Culture Collection, VA, USA) were seeded in a 24 well plate ($\sim 10^4$), allowed to attach overnight and treated after 24 and 72 h with vehicle (DMSO), various concentrations of paclitaxel (1 nM to 100 μ M), GYY4137 (1 nM to 100 μ M) or a combination of both drugs. Growth was assessed by MTT [3-(4,5-dimethylthiazol-2-yl)-2,5-diphenyltetrazolium bromide] assay (Promega, Madison, USA) after 96 h of incubation. The concentration of either drug that gave half-maximal response (IC₅₀) was calculated using non-linear regression analysis. The data were fitted to a dose-response-inhibition equation (log [inhibitor] vs. normalized response curve).

2.11. Statistical analysis

The software GraphPad Prism version 6.00 (GraphPad Software Inc., USA) was used for data and statistical analyses. Statistical analyses were performed using unpaired Student's *t* test, one-way analysis of variance (ANOVA) followed by Bonferroni's multiple comparison post-tests, Kruskal-Wallis test followed by Dunn's multiple comparison test and two-way repeated ANOVA followed by Bonferroni's multiple comparison post-tests. For Fig. 1A, which has several time points and groups, the experimental design was such that data were arranged as follows: each row represented a different time point and each column represented a treatment group, so matched values were stacked into a subcolumn. Based on this a repeated measures two-way ANOVA was performed. This was followed by a post analysis for correction of multiple comparisons with Bonferroni's test (CIs and significance were

computed) where within each row, columns were compared (simple effects within each row) i.e. compared each cell mean with every other cell mean on that row. The differences were considered significant when $p < 0.05$. The results were expressed as the mean \pm standard error of the mean (S.E.M).

3. Results

3.1. GYY4137 alleviates established paclitaxel-induced thermal hyperalgesia in an ATP sensitive potassium channel (K_{ATP} channel)-dependent manner

At the baseline day (day 0), there were no significant differences in the withdrawal latencies to heat-stimuli between the animal groups. Paclitaxel-treated mice had significant reduction in RTL (thermal hyperalgesia) in the hot plate test on day 7 after first drug administration compared to the baseline (pretreatment) latency (Fig. 1A; $p < 0.05$). Therefore, paclitaxel-treated mice developed thermal hyperalgesia on day 7 after first administration of paclitaxel, in agreement with previous evidence [17]. The positive analgesic control drug gabapentin (10 mg/kg) produced antihyperalgesic effect starting after 1.5 h of treatment, i.e. significantly increasing RTL to 5.2 ± 0.2 s, as compared to 3.6 ± 0.2 s for paclitaxel + vehicle group ($n = 6$; $p < 0.05$, Fig. 1A). The antihyperalgesic effect of gabapentin was from 1.5 to 3 h, reached a peak level after 2 h (RTL 6.1 ± 0.2 s vs. 3.6 ± 0.2 s for paclitaxel + vehicle group; $n = 6$; $p < 0.01$, Fig. 1A). Treatment with GYY4137 produced antihyperalgesic effects with all the tested doses but with variable start and peak times. A 25 mg/kg dose of GYY4137 produced a significant antihyperalgesic effect from 1.5 to 3 h after treatment, as evident by the increased RTL to 5.4 ± 0.1 s ($n = 8$) compared to 3.5 ± 0.2 s for paclitaxel + vehicle group at 1.5 h and 5.5 ± 0.4 ($n = 8$) compared to 3.7 ± 0.2 s for paclitaxel + vehicle group ($n = 6$) at 3 h ($p < 0.01$; Fig. 1A) and reached a peak at 2 h (RTL 6.8 ± 0.2 s, $n = 8$ vs. 3.6 ± 0.2 , $n = 6$ paclitaxel + vehicle-treated mice; $p < 0.001$; Fig. 1A). A 50 mg/kg dose of GYY4137 produced antihyperalgesic effect from 1 to 2 h; RTL of 5.2 ± 0.3 s ($n = 8$) compared to 3.4 ± 0.3 s ($n = 6$) for paclitaxel + vehicle-treated mice ($p < 0.05$; Fig. 1A) at 1 h, and peaked and ended at 2 h with RTL of 7.1 ± 0.1 s ($n = 8$) compared to 3.6 ± 0.2 s ($n = 6$) for paclitaxel + vehicle-treated mice ($p < 0.01$; Fig. 1). The highest tested GYY4137 dose (100 mg/kg) also significantly increased the RTL compared to paclitaxel + vehicle-treated mice from 1 to 4 h (when the experiment was terminated): RTL 5.1 ± 0.2 s ($n = 8$) vs. 3.4 ± 0.3 s for paclitaxel + vehicle-treated mice ($n = 6$) at 1 h ($p < 0.05$; Fig. 1A), peaked at 3 h (RTL 7.2 ± 0.3 s, $n = 8$ vs. 3.7 ± 0.2 , $n = 6$, respectively; $p < 0.01$; Fig. 1), and remained significantly high until 4 h (RTL 4.7 ± 0.2 s, $n = 8$ vs. 3.1 ± 0.3 , $n = 6$, respectively; $p < 0.01$; Fig. 1A). A significant difference was observed in the therapeutic effects of gabapentin 10 mg/kg and GYY4137 100 mg/kg only against paclitaxel-induced thermal hyperalgesia at 3 h (RTL 5.8 ± 0.4 s, $n = 8$ for gabapentin 10 mg/kg vs. 7.2 ± 0.3 , $n = 6$ for GYY4137 100 mg/kg; $p < 0.05$). The other difference was in the starting time of induction of antihyperalgesic effect, as GYY4137 100 mg/kg induced its antihyperalgesic action earlier (after 1 h) than gabapentin (after 1.5 h), and the effect was sustained for a longer time (up to 4 h) for GYY4137 compared to 3 h only with gabapentin 10 mg/kg (Fig. 1A).

The optimal time point (2 h) and dose (50 mg/kg) for GYY4137 analgesic activity were selected based on the results from the dose- and time-response experiment depicted in Fig. 1. The administration of the K_{ATP} channel antagonist glibenclamide (10 mg/kg) to mice with paclitaxel-induced thermal hyperalgesia did not alter the reaction latency to hot-plate test compared to vehicle-treated mice ($p > 0.05$; Fig. 1B). However, treatment with glibenclamide significantly attenuated the antihyperalgesic effect of GYY4137 in the mice, i.e. a 37 % reduction in reaction latency from 8.1 ± 0.3 s for paclitaxel + GYY4137 to 5.2 ± 0.1 s for paclitaxel + GYY4137 + glibenclamide ($p < 0.01$; Fig. 1B). This result reveals that the acute antihyperalgesic action of

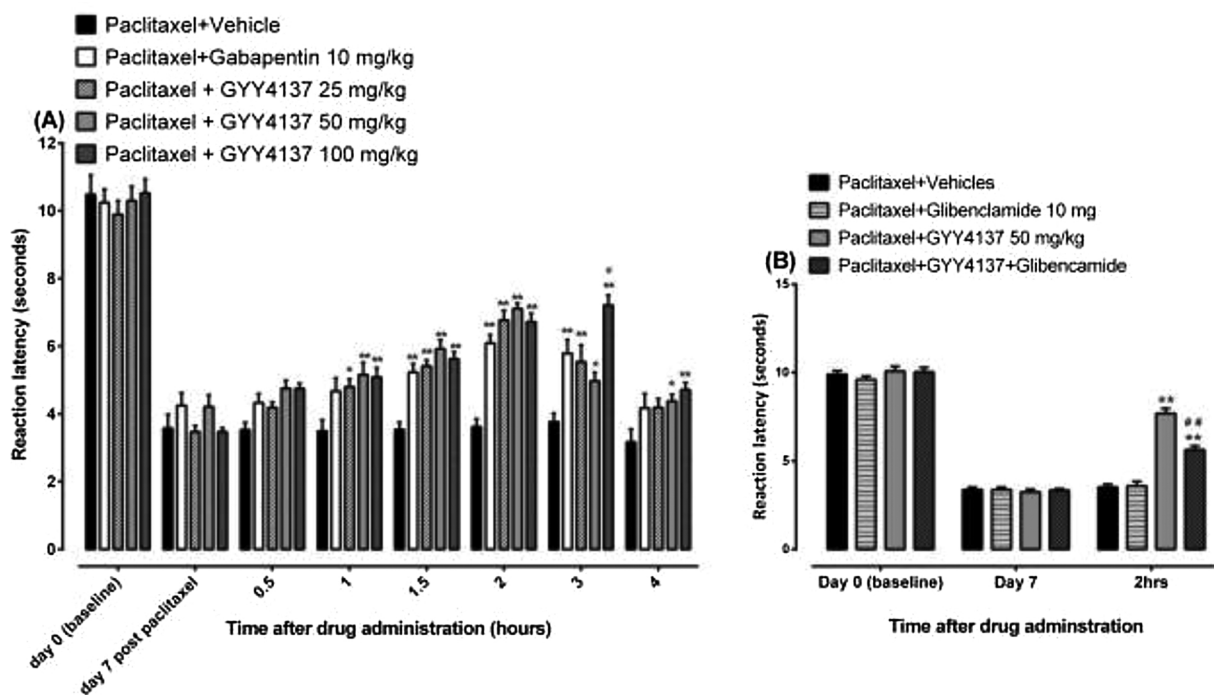


Fig. 1. Antihyperalgesic effects of GYY4137 against established paclitaxel-induced thermal hyperalgesia in female BALB/c mice is blocked by an ATP sensitive potassium channel (K_{ATP} channel) inhibitor. (A) Effect of treatment with GYY4137 and gabapentin on mice with paclitaxel-induced thermal hyperalgesia in a hot-plate test. Reaction latencies (seconds) were recorded from baseline values (taken before and at day 7 after first administration of paclitaxel) and at different time points following treatment with gabapentin (10 mg/kg), GYY4137 (25, 50 and 100 mg/kg), or their vehicles. Each bar represents the mean \pm S.E.M (n = 6-8). * $p < 0.05$, ** $p < 0.01$ compared to paclitaxel vehicle, # $p < 0.05$ compared to gabapentin at the same time point after treatment. (B) Effect of treatment with GYY4137 and glibenclamide, a K_{ATP} channel inhibitor, on mice with paclitaxel-induced thermal hyperalgesia in a hot-plate test. Reaction latencies (seconds) were recorded from baseline values (taken before and at day 7 after first administration of paclitaxel) and after 2 h following treatment with glibenclamide (10 mg/kg), GYY4137 (50 mg/kg), combination of GYY4137 and glibenclamide, or their vehicles. Each bar represents the mean \pm S.E.M. (n = 9). *** $p < 0.001$ compared to drug vehicle, ### $p < 0.001$ compared to GYY4137-treated group.

GYY4137 is dependent, at least partly, on K_{ATP} channels.

3.2. Coadministration of paclitaxel with GYY4137 prevents the development of paclitaxel-induced thermal hyperalgesia, cold allodynia and mechanical allodynia

Mice treated with paclitaxel plus GYY4137 (50 mg/kg) had RTL (8.22 ± 0.5 s, n = 10) similar to the vehicle-only treated control animals without hyperalgesia (9.29 ± 0.2 s, n = 8; $p > 0.05$; Fig. 3), which were significantly higher than those of the mice treated with paclitaxel alone. As such, the RTL of the mice co-treated with paclitaxel plus GYY4137 at 50 mg/kg for 5 consecutive days was significantly higher on day 7 after the first drug administration than those treated with paclitaxel alone, i.e. with hyperalgesia (RTL 8.22 ± 0.5 vs. 5.67 ± 0.2 s, respectively, n = 10; $p < 0.0001$; Fig. 2A). Similar results in mice co-treated with paclitaxel and GYY4137 (50 mg/kg) were observed following assessment of cold and mechanical allodynia (Fig. 2B & C). In the cold plate test, the RTL of paclitaxel + GYY4137-treated animals was significantly higher compared to paclitaxel-treated animals (RTL 50.09 ± 3.9 vs 26.04 ± 2.0 s, n = 8, respectively; $p < 0.001$; Fig. 2B) and was similar to the vehicle-only treated group (RTL 55.86 ± 1.5 s, n = 8; $p > 0.05$; Fig. 2B). In a separate set of experiments, paclitaxel + GYY4137 treated animals showed significantly higher withdrawal threshold to mechanical stimuli than paclitaxel-treated mice (3.27 ± 0.07 g vs 1.82 ± 0.08 g, respectively; n = 8; $p < 0.001$; Fig. 2C), but was similar to the vehicle-only treated group (3.7 ± 0.1 g, n = 8; $p > 0.05$; Fig. 2C). These data show that the concomitant treatment of paclitaxel with GYY4137 markedly prevented the development of paclitaxel-induced thermal hyperalgesia as well as cold and mechanical allodynia, thus indicating a preventive/

prophylactic effect of GYY4137.

3.3. Effect of treatment with paclitaxel or paclitaxel plus GYY4137 on H_2S level in plasma and H_2S generated by enzymes in tissues

Plasma H_2S levels were not different in paclitaxel-treated group compared to control (untreated) animals, but were significantly increased in mice co-treated with paclitaxel plus GYY4137 compared to control animals or paclitaxel-treated group ($p < 0.05$; Fig. 3A) on day 7 after first drug administration. H_2S generated by enzymes in the brain was similar in all the three groups i.e. control, paclitaxel-treated and paclitaxel plus GYY4137 co-treated groups ($p > 0.05$; Fig. 3B) on day 7 after first drug administration. On the other hand, H_2S generated by enzymes in the spinal cord and paw skin was significantly lower in paclitaxel-treated mice than in untreated control mice ($p < 0.05$; Fig. 3C-D), and co-treatment with paclitaxel plus GYY4137 significantly increased H_2S generation compared to paclitaxel only-treated mice ($p < 0.05$; Fig. 3C-D).

3.4. GYY4137 enhances the anti-proliferative effects of paclitaxel

The exposure of cultured breast cancer MCF-7 cells to paclitaxel (1 nM to 100 μ M) for 96 h caused concentration-dependent decrease in tumor cell viability as assessed by MTT assay ($p < 0.05$; Fig. 4A). Paclitaxel inhibited MCF-7 cell proliferation by 40 % at 10 nM concentration which was increased to 50 % at concentrations ranging from 50 nM to 10 μ M. At higher concentrations (50–100 μ M) paclitaxel almost completely inhibited cell proliferation. The IC_{50} of paclitaxel was 80 nM. GYY4137 did not inhibit cell proliferation at concentrations ranging from 1 nM to 50 μ M, but significantly inhibited (40 %) cell

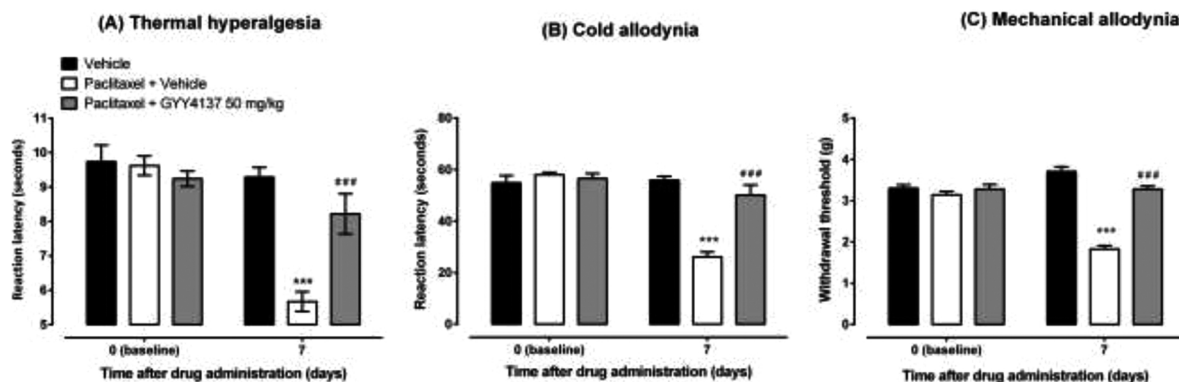


Fig. 2. Co-administration of GYY4137 with paclitaxel prevents the development of paclitaxel-induced thermal hyperalgesia, cold allodynia and mechanical allodynia in female BALB/c mice. Effect of co-administration of GYY4137 with paclitaxel on the development of (A) paclitaxel-induced thermal hyperalgesia in a hot-plate test, (B) paclitaxel-induced cold allodynia in a cold-plate test and (C) paclitaxel-induced mechanical allodynia measured by a dynamic plantar aesthesiometer. Paclitaxel (2 mg/kg) was administered for 5 days with vehicle or GYY4137 (50 mg/kg). Each bar represents the mean \pm S.E.M (n = 8-12). *** p < 0.001 compared to vehicles only group (without hyperalgesia/allodynia) at the same time point after treatment. ### p < 0.001 compared to mice treated with paclitaxel-induced hyperalgesia/allodynia treated with vehicle.

proliferation at 100 μ M concentration (p < 0.05; Fig. 4A). GYY4137 (100 μ M) produced an antitumor effect in MCF-7 cell line, in agreement with previously published reports [18]. The IC₅₀ of GYY4137 was 373 μ M. The combination regimen of paclitaxel (50 nM) plus GYY4137 (100 μ M) significantly inhibited cell proliferation compared with monotherapy (Fig. 4B). GYY4137 increased the paclitaxel-induced decrease

of cell viability of this breast carcinoma cell line (Fig. 4B). The combination of GYY4137 (100 μ M) plus paclitaxel (50 nM) decreased the tumor cell proliferation significantly much more than each individual drug (p < 0.05; Fig. 4B). Thus, the combination of paclitaxel plus GYY4137 does not negatively interfere with the anti-proliferative activity of paclitaxel in breast cancer cell line *in vitro*; rather, produces a

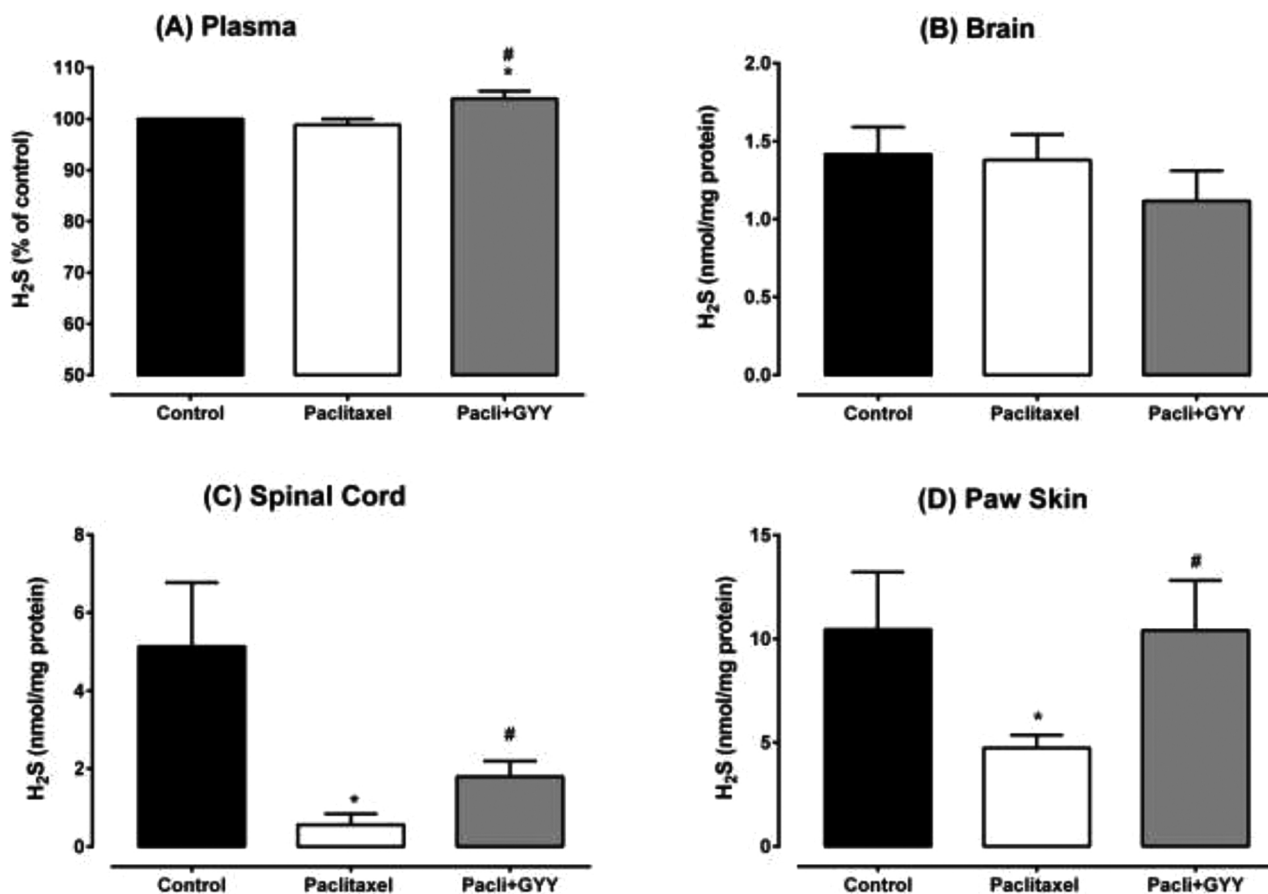


Fig. 3. Measurement of H₂S level in control (untreated), paclitaxel-treated and paclitaxel and GYY4137 (50 mg/kg) co-treated mice at day 7 after first administration of paclitaxel. (A) Plasma H₂S levels were not different in paclitaxel group compared to control animals, but were significantly increased with GYY4137 co-treatment compared to both control (* p < 0.05) and paclitaxel only group (# p < 0.05). (B) Brain H₂S enzymatic generation is similar in all the groups (p > 0.05). (C) Spinal cord and (D) paw skin H₂S enzymatic production in paclitaxel-treated mice is significantly lower than untreated controls (* p < 0.05), and GYY4137 co-treatment significantly increased spinal cord H₂S generation compared to paclitaxel only-treated mice (# p < 0.05). Bars represent mean \pm S.E.M of 6-8 samples.

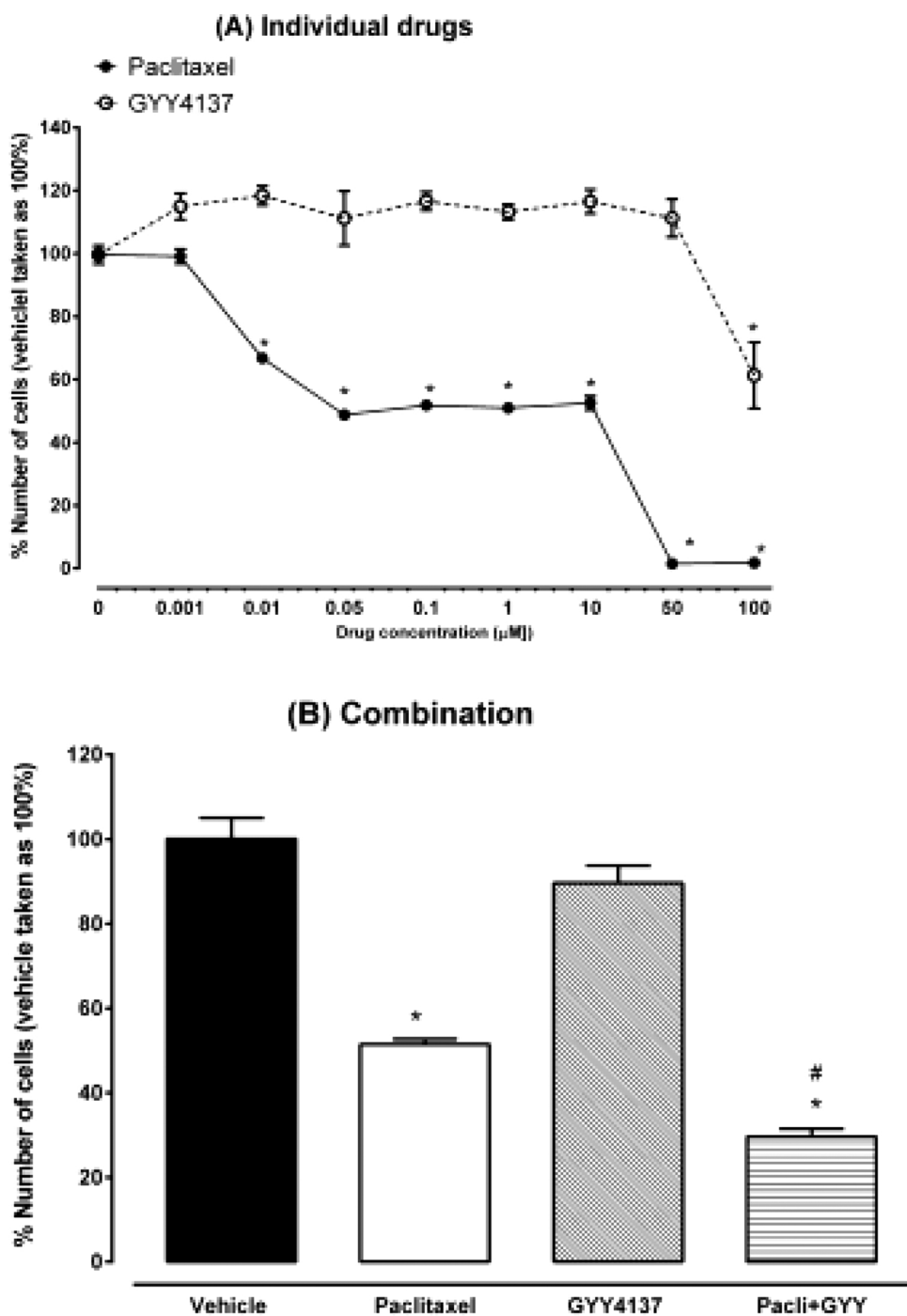


Fig. 4. Effects of monotherapy or combination regimen with paclitaxel or GYY on MCF-7 cell proliferation. Cells were seeded in a 24 well plate, allowed to attach overnight and treated after 24 and 72 h with vehicle (solid bars) or various concentrations of (A) paclitaxel and GYY4137 or (C) their combination. Growth was assessed by MTT assay after 96 h of incubation. Each point or bar represents the mean ± SEM of 3 determinations. * p < 0.05 denote significant difference from vehicle-treated group (0 in figure A), # p < 0.05 denote significant difference from paclitaxel monotherapy.

positive additive anti-proliferative effect.

4. Discussion

The findings of the present study suggest that the slow release H₂S donor GYY4137 has therapeutic potential and preventive role of in CINP caused by paclitaxel in a murine model. GYY4137 produced an acute antihyperalgesic effect comparable to the anticonvulsant gabapentin, which is commonly used to relieve neuropathic pain. The antihyperalgesic effect of GYY4137 was antagonized by the K_{ATP} channel

blocker glibenclamide. Co-administration of GYY4137 with paclitaxel prevented the development of paclitaxel-induced thermal hyperalgesia, cold allodynia and mechanical allodynia. Paclitaxel-treatment induced a decrease in H₂S generation by enzymes in the paw skin and spinal cord, which was prevented by co-administration with GYY4137. GYY4137 had some anti-proliferative effects against a breast cancer cell line MCF-7 and enhanced the anti-proliferative effects of paclitaxel against these cells.

The antihyperalgesic effect of GYY4137 in mice with established paclitaxel-induced thermal hyperalgesia was comparable to that of

gabapentin, although the highest dose of GYY4137 used (100 mg/kg) produced a higher effect at one-time point (3 h) and had an earlier onset and longer duration of antihyperalgesic activity than gabapentin from 1 to 4 h versus from 1.5 to 3 h, respectively. Gabapentin has been reported to ameliorate several types of acute and chronic pain [22] including diabetic neuropathic pain [23] and CINP [24–27]. The results of the current study demonstrate that GYY4137 has antihyperalgesic activities against paclitaxel-induced thermal hyperalgesia. GYY4137 and another H₂S donor NaHS have also been shown to relieve cold allodynia induced by another anticancer drug oxaliplatin in mice [13]. NaHS also relieved cold allodynia induced by paclitaxel in mice [13]. Hydrogen sulfide donors have been reported to alleviate other types of neuropathic pain such as neuropathic pain in chronic constriction injured rats [10]. The activity of NaHS against oxaliplatin-induced cold-allodynia was inhibited by the Kv7 potassium channel blocker XE991 [13], demonstrating a role of the voltage-gated Kv7 potassium channels in the antiallodynic effect of H₂S donors. There are many types of potassium channels that fall under four classes: calcium-activated potassium channels, inwardly rectifying potassium channels, tandem pore domain potassium channels and voltage-gated potassium channels. The involvement of potassium channels activation in mediating analgesia has been demonstrated for several drugs, such as opioids [27], some nonsteroidal anti-inflammatory drugs (NSAIDs) [28], and the antidepressants amitriptyline and clomipramine [29]. Previous studies in inflammatory pain models showed that the H₂S-releasing aspirin (NOSH-aspirin) was superior to aspirin in reducing inflammatory pain [30], possibly due to H₂S inhibiting the production of pronociceptive cytokines such as IL-1 β , and directly blocking certain hyperalgesic mediators in a mechanism dependent on modulation of K_{ATP} channels [30]. Various studies have shown that H₂S also produces its effects via activation of K_{ATP} channel, an inwardly rectifying potassium channel [31]. In the current study, the antihyperalgesic activity of GYY4137 against paclitaxel-induced thermal hyperalgesia was blocked by the K_{ATP} channel blocker glibenclamide, demonstrating a role of K_{ATP} channel in the antiallodynic effect of the H₂S donor. A similar effect was also reported in the gastrointestinal tract as H₂S was shown to exert antinociceptive activity by activating K_{ATP} channels [32].

H₂S levels and expression of the H₂S-generating enzymes have been found to be altered in plasma and tissues of animal models of various diseases including atherosclerosis, diabetes, diabetic cardiomyopathy, traumatic brain injury (TBI) etc. [33–37]. Thus, we determined H₂S level in the plasma, and the enzyme-mediated H₂S generation in isolated brain, spinal cord and paw skin tissues from paclitaxel-treated mice suffering from painful neuropathy to understand its possible implication in the pathogenesis of CINP. Mice with established paclitaxel-induced hyperalgesia and allodynia did not exhibit any change in plasma H₂S level or brain H₂S generation, however spinal cord and paw skin H₂S generation was significantly reduced. These findings suggest that deficiency in H₂S generation in both the central nervous system i.e. spinal cord and the periphery i.e. paw skin might contribute to the pathogenesis of paclitaxel-induced hyperalgesia and allodynia. Co-treatment with GYY4137 prevented the reduction in H₂S generation induced by paclitaxel as well as the paclitaxel-induced thermal hyperalgesia, cold allodynia and mechanical allodynia. This suggest that prevention of chemotherapy-induced reduction in H₂S generation using H₂S donors such as GYY4137 is a plausible therapeutic option for CINP. This is similar to what has been reported in an animal model of TBI, where using NaHS as an H₂S donor protected against brain edema, behavior deficits and brain damage induced by TBI [38].

Paclitaxel is used as a chemotherapeutic drug and therefore it is preferable that any drug used to alleviate its adverse effects should not negatively impact the anticancer effect of paclitaxel. GYY4137 has been reported to have anti-cancer activities both *in vitro* and *in vivo* [21,39,40]. In the current study, GYY4137 also had anti-proliferative activity against MCF-7, a breast cancer cell line, similar to what was previously described [21]. GYY4137 enhanced the anti-proliferative

properties of paclitaxel against the MCF-7 cell line. These results suggest that GYY4137 in addition to alleviation and prevention of paclitaxel-induced painful neuropathy it also enhances paclitaxel's anti-proliferative properties against a cancer cell line, and therefore may be useful for the prevention and management of paclitaxel-induced painful neuropathy.

5. Conclusion

In conclusion, the results of the current study reveal for the first time that the slow-release H₂S donor GYY4137 can both prevent the development of paclitaxel-induced neuropathic pain (PINP) and alleviate established PINP, while enhancing paclitaxel's anti-proliferative properties against a cancer cell line. These findings support previous reports demonstrating the ability of H₂S to ameliorate allodynia and hyperalgesia associated with other types of neuropathic pain in animal models [9–12]. Deficiency in the generation of the endogenous H₂S seems to play a role in the pathogenesis of PINP. Further studies are necessary to investigate the changes in H₂S generating enzymes and their possible contribution to PINP or CINP in general. GYY4137 and possibly other slow-release H₂S donors warrant further research as potential drugs for prevention or alleviation of PINP in order to improve the outcomes and quality of life for patients receiving paclitaxel as a chemotherapeutic drug.

Declaration of Competing Interest

There is no conflict of interests, financial or any other, in this study.

Acknowledgment

This study was funded by Kuwait University, Research Administration, Project No. PT04/16. We also would like to acknowledge "General Facilities Science (GF-S), Faculty of Science Nos. GS01/03 (GC MS DFS - Thermo and Bruker 600 MHz NMR) and GS02/10 (LC-MS/MS - Waters QToF)".

References

- [1] R.H. Dworkin, M. Backonja, M.C. Rowbotham, R.R. Allen, C.R. Argoff, G.J. Bennett, M.C. Bushnell, J.T. Farrar, B.S. Galer, J.A. Haythornthwaite, D.J. Hewitt, J.D. Loeser, M.B. Max, M. Saltarelli, K.E. Schmader, C. Stein, D. Thompson, D.C. Turk, M.S. Wallace, L.R. Watkins, S.M. Weinstein, Advances in neuropathic pain: diagnosis, mechanisms, and treatment recommendations, *Arch. Neurol.* 60 (2003) 1524–1534.
- [2] P. Honore, Behavioral assessment of neuropathic pain in preclinical models, *Drug Dev. Res.* 67 (2006) 302–307.
- [3] E. Esin, S. Yalcin, Neuropathic cancer pain: What we are dealing with? How to manage it? *Oncol. Ther.* 7 (2014) 599–618.
- [4] D.L. Hershman, C. Lacchetti, R.H. Dworkin, et al., Prevention and management of chemotherapy-induced peripheral neuropathy in survivors of adult cancers: american Society of Clinical Oncology clinical practice guideline, *J. Clin. Oncol.* 32 (June (18)) (2014) 1941–1967, <https://doi.org/10.1200/jco.2013.54.0914>.
- [5] Kim PY, Johnson CE, Chemotherapy-induced peripheral neuropathy: a review of recent findings, *Curr. Opin. Anaesthesiol.* (October;30(5)) (2017) 570–576, <https://doi.org/10.1097/aco.0000000000000500>.
- [6] H. Kimura, Hydrogen sulfide: from brain to gut, *Antioxid. Redox Signal.* 12 (2010) 1111–1123.
- [7] S. Panthi, H.J. Chung, J. Jung, N.Y. Jeong, Physiological importance of hydrogen sulfide: emerging potent neuroprotector and neuromodulator, *Oxid. Med. Cell. Longev.* (2016) 9049782.
- [8] R. Wang, Physiological implications of hydrogen sulfide: a whiff exploration that blossomed, *Physiol. Rev.* 92 (2012) 791–896.
- [9] K. Kida, E. Marutani, R.K. Nguyen, F. Ichinose, Inhaled hydrogen sulfide prevents neuropathic pain after peripheral nerve injury in mice, *Nitric Oxide—Biol. Chem.* 46 (2015) 87–92.
- [10] J. Lin, H. Luo, C. Lin, J. Chen, X. Lin, Sodium hydrosulfide relieves neuropathic pain in chronic constriction injured rats, *Evid. Based Complement. Altern. Med.* 2014 (2014) 7. Article ID 514898.
- [11] M.D. Fonseca, F.Q. Cunha, K. Kashfi, Cunha TM. NOSH-aspirin (NBS-1120), a dual nitric oxide and hydrogen sulfide-releasing hybrid, reduces inflammatory pain, *Pharmacol. Res. Perspect.* 3 (3) (2015) e00133-n/a.
- [12] E. Distrutti, S. Cipriani, B. Renga, et al., Hydrogen sulphide induces micro opioid

- receptor-dependent analgesia in a rodent model of visceral pain, *Mol. Pain* 6 (June 11) (2010) 36, <https://doi.org/10.1186/1744-8069-6-36> Published 2010.
- [13] L. Di Cesare Mannelli, E. Lucarini, L. Micheli, I. Mosca, P. Ambrosino, M.V. Soldovieri, A. Martelli, L. Testai, M. Tagliatalata, V. Calderone, C. Ghelardini, Effects of natural and synthetic isothiocyanate-based H₂S-releasers against chemotherapy-induced neuropathic pain: role of Kv7 potassium channels, *Neuropharmacology* (2017), <https://doi.org/10.1016/j.neuropharm.2017.04.029>.
- [14] L. Li, M. Whiteman, Y.Y. Guan, K.L. Neo, Y. Cheng, S.W. Lee, Y. Zhao, R. Baskar, C.H. Tan, P.K. Moore, Characterization of a novel, water-soluble hydrogen sulfide-releasing molecule (GYY4137): new insights into the biology of hydrogen sulfide, *Circulation* 117 (18) (2008) 2351–2360.
- [15] M. Zimmermann, Ethical guidelines for investigations of experimental pain in conscious animals, *Pain* 16 (1983) 109–110.
- [16] C. Kilenny, W.J. Browne, I.C. Cuthill, M. Emerson, D.G. Altman, Improving bioscience research reporting: the ARRIVE guidelines for reporting animal research, *J. Pharmacol. Pharmacother.* 1 (2010) 94–99.
- [17] S. Parvathy, W. Masocha, Matrix metalloproteinase inhibitor COL-3 prevents the development of paclitaxel-induced hyperalgesia in mice, *Med. Princ. Pract.* 22 (2013) 35–41.
- [18] F.R. Nieto, J.M. Entrena, C.M. Cendán, E.D. Pozo, J.M. Vela, J.M. Baeyens, Tetrodotoxin inhibits the development and expression of neuropathic pain induced by paclitaxel in mice, *Pain* 137 (2007) 520–531.
- [19] S.J. Ward, M.D. Ramirez, H. Neelakantam, E.A. Walker, Cannabidiol prevents the development of cold and mechanical allodynia in paclitaxel-treated female C57Bl6 mice, *Anesth. Analg.* 113 (2011) 947–950.
- [20] D. Thangamani, I.O. Edafogho, W. Masocha, The anticonvulsant enaminone E139 attenuates paclitaxel-induced neuropathic pain in rodents, *ScientificWorldJournal*. (2013 December 8) (2013) 240508, <https://doi.org/10.1155/2013/240508> Published 2013.
- [21] Z.W. Lee, J. Zhou, C.S. Chen, et al., The slow-releasing hydrogen sulfide donor, GYY4137, exhibits novel anti-cancer effects in vitro and in vivo, *PLoS One* 6 (6) (2011) e21077, <https://doi.org/10.1371/journal.pone.0021077>.
- [22] P.J. Wiffen, H.J. McQuay, J.E. Edwards, R.A. Moore, Gabapentin for acute and chronic pain, *Cochrane Database Syst. Rev.* (July 20; (3)) (2005) CD005452, <https://doi.org/10.1002/14651858.CD005452> Published online 2005 Jul 20.
- [23] B. Hemstreet, M. Lapointe, Evidence for the use of gabapentin in the treatment of diabetic peripheral neuropathy, *Clin. Ther.* 23 (April (4)) (2001) 520–531.
- [24] W. Xiao, A. Boroujerdi, G.J. Bennett, Z.D. Luo, Chemotherapy-evoked painful peripheral neuropathy: analgesic effects of gabapentin and effects on expression of the alpha-2-delta type-1 calcium channel subunit, *Neuroscience* 144 (2) (2007) 714–720, <https://doi.org/10.1016/j.neuroscience.2006.09.044>.
- [25] J. Guindon, Y. Lai, S.M. Takacs, H.B. Bradshaw, A.G. Hohmann, Alterations in endocannabinoid tone following chemotherapy-induced peripheral neuropathy: effects of endocannabinoid deactivation inhibitors targeting fatty-acid amide hydrolase and monoacylglycerol lipase in comparison to reference analgesics following cisplatin treatment, *Pharmacol. Res.* 67 (1) (2013) 94–109, <https://doi.org/10.1016/j.phrs.2012.10.013>.
- [26] M. Zhao, et al., Pharmacological characterization of standard analgesics on oxaliplatin-induced acute cold hypersensitivity in mice, *J. Pharmacol. Sci.* 124 (2014) 514–517, <https://doi.org/10.1254/jphs.13249SC>.
- [27] S.P. Welch, L.D. Dunlow, Antinociceptive activity of intrathecally administered potassium channel openers and opioid agonists, a common mechanism of action? *J. Pharmacol. Exp. Ther.* 267 (1993) 390–399.
- [28] Y. Mi, X. Zhang, F. Zhang, et al., The role of potassium channel activation in celecoxib-induced analgesic action, *PLoS One* 8 (1) (2013) e54797, <https://doi.org/10.1371/journal.pone.0054797>.
- [29] N. Galeotti, C. Ghelardini, A. Bartolini, Involvement of potassium channels in amitriptyline and clomipramine analgesia, *Neuropharmacology* 40 (2001) 75–84.
- [30] M.D. Fonseca, F.Q. Cunha, K. Kashfi, Cunha TM. NOSH-aspirin (NBS-1120), a dual nitric oxide and hydrogen sulfide-releasing hybrid, reduces inflammatory pain, *Pharmacol. Res. Perspect.* 3 (3) (2015) e00133, <https://doi.org/10.1002/prp2.133>.
- [31] W. Guo, Z.Y. Cheng, Y.Z. Zhu, Hydrogen sulfide and translational medicine, *Acta Pharmacol. Sin.* 34 (10) (2013) 1284–1291, <https://doi.org/10.1038/aps.2013.127>.
- [32] E. Distrutti, L. Sediari, A. Mencarelli, B. Renga, S. Orlandi, E. Antonelli, et al., Evidence that hydrogen sulfide exerts antinociceptive effects in the gastrointestinal tract by activating K_{ATP} channels, *J. Pharmacol. Exp. Ther.* 316 (1) (2006) 325–335.
- [33] M. Zhang, H. Shan, T. Wang, et al., *Neurochem. Res.* 38 (2013) 714, <https://doi.org/10.1007/s11064-013-0969-4>.
- [34] S. Jin, S.X. Pu, C.L. Hou, et al., Cardiac H₂S generation is reduced in ageing diabetic mice, *Oxid. Med. Cell. Longev.* 2015 (2015) 758358, <https://doi.org/10.1155/2015/758358>.
- [35] S.K. Jain, R. Bull, J.L. Rains, et al., Low levels of hydrogen sulfide in the blood of diabetes patients and streptozotocin-treated rats causes vascular inflammation? *Antioxid. Redox Signal.* 12 (11) (2010) 1333–1337, <https://doi.org/10.1089/ars.2009.2956>.
- [36] S.K. Jain, P. Manna, D. Micinski, et al., In African American type 2 diabetic patients, is vitamin D deficiency associated with lower blood levels of hydrogen sulfide and cyclic adenosine monophosphate, and elevated oxidative stress? *Antioxid. Redox Signal.* 18 (10) (2013) 1154–1158, <https://doi.org/10.1089/ars.2012.4843>.
- [37] S. Mani, H. Li, A. Untereiner, L. Wu, G. Yang, R.C. Austin, J.D. Dickhout, S. Lhotak, Q.H. Meng, R. Wang, Decreased endogenous production of hydrogen sulfide accelerates atherosclerosis, *Circulation* 127 (2013) 2523–2534.
- [38] M. Zhang, H. Shan, P. Chang, et al., Hydrogen sulfide offers neuroprotection on traumatic brain injury in parallel with reduced apoptosis and autophagy in mice, *PLoS One* 9 (January 23 (1)) (2014) e87241, <https://doi.org/10.1371/journal.pone.0087241> Published 2014.
- [39] S. Lu, Y. Gao, X. Huang, Wang X. GYY4137, A hydrogen sulfide (H₂S) donor, shows potent anti-hepatocellular H₂S IN CANCER BIOLOGY AND THERAPY 31 carcinoma activity through blocking the STAT3 pathway, *Int. J. Oncol.* 44 (2014) 1259–1267.
- [40] S. Sakuma, S. Minamino, M. Takase, et al., Hydrogen sulfide donor GYY4137 suppresses proliferation of human colorectal cancer Caco-2 cells by inducing both cell cycle arrest and cell death, *Heliyon* 5 (August 9 (8)) (2019) e02244, <https://doi.org/10.1016/j.heliyon.2019.e02244> Published 2019.